Mathematical models and numerical simulations of a thermally expandable microballoon for plastic foaming

AUTHOR(S):

Fujino, Masayasu; Taniguchi, Takashi; Kawaguchi, Yasuhiro; Ohshima, Masahiro

CITATION:

Fujino, Masayasu ...[et al]. Mathematical models and numerical simulations of a thermally expandable microballoon for plastic foaming. Chemical Engineering Science 2013, 104: 220-227

ISSUE DATE:

2013-12

URL:

http://hdl.handle.net/2433/179293

MATHEMATICAL MODELS AND NUMERICAL SIMULATIONS OF A THERMALLY EXPANDABLE MICROBALLOON FOR PLASTIC FOAMING

Masayasu Fujino[1], Takashi Taniguchi[1], Yasuhiro Kawaguchi[2] and Masahiro Ohshima*[1],

1. Dept. of Chemical Engineering, Kyoto University, Kyoto 61- 8510, Japan

2. Technical Section, Polymer production Dept., Tokuyama Sekisui CO.,LTD. Yamaguchi, 746-0006, Japan

* corresponding author: oshima@cheme.kyoto-u.ac.jp +81-75-383-2666

Abstract

Thermally expandable microcapsules, often called microspheres or microballoons, are utilized in compression, injection molding and extrusion processes to foam different types of polymers. Microballoons consist of a polymer shell and a liquid hydrocarbon core. Hydrocarbons are used as a physical blowing agent. In this study, a mathematical model was developed to describe the expansion behavior of a microballoon in air and in a polymer matrix. The model was used to determine the key factors in improving the expandability of the balloon at designated temperatures. The viscoelastic properties of the polymer shell, evaporation of hydrocarbons in the balloon and diffusion behavior of the blowing agent through the polymer shell were taken into account in the model. The results of the developed

model showed quite good agreement with the experimentally observed thermal expansion behavior of a microballoon. ~~A~~ sensitivity analysis of the expansion behavior with respect to the properties of the microballoon was also conducted to devise an optimal design strategy for high-expansion microballoons.

Keywords; microballoon, microsphere, expandability, mathematical modeling, Polymer processing, viscoelasticity.

1. INTRODUCTION

Recently, requirements for further reducing the weight of plastic parts, especially automotive parts for mileage improvement, have been established. Plastic parts other than those used in the automotive industry also require a reduction in weight without deteriorating their mechanical properties and appearance. Polymer foaming is one of the most promising techniques for realizing weight reduction. Polymer foaming methods can be roughly divided into two groups: chemical foaming and physical foaming. Chemical foaming uses chemicals that release gas, such as carbon dioxide (CO_2) and nitrogen (N_2), by thermal decomposition. The released gas dissolves into the polymer or directly leads to bubble expansion and the formation of a cellular structure. Physical foaming does not involve any chemical reaction. It simply uses butane, pentane, CO_2 or N_2 as a blowing agent.

Thermally expandable microballoons are used in physical foaming, in which polymeric capsules are used to foam polymers. A low-boiling-point hydrocarbon liquid, such as octane or pentane, is encapsulated by a polymeric shell. By mixing microballoons with a thermoplastic polymer and allowing them to thermally expand, the polymers can be foamed. When microballoons are heated, they expand to 50–100 times their initial volumes.

The polymeric microballoon was originally developed by Dow Chemical Co. (Morehouse et al, 1964) and has been advanced by others (Lundqvist, 1992, Yokomizo, et al, 1997).

Nowadays, microballoons are available in a variety of grades (Jonsson 2006), and have been used in car parts (Mae et al, 2008 a,b) , shoe sole production, vinyl plastisol formulations (Ahmad et al, 2001), as well as the rotational molding of linear low-density polyethylene and ethylene-vinyl acetate (Takacs, et al. 2002, D'Agostino et al, 2003). Even though there a large number of patents and application reports have been issued, scientific papers, which discussed the synthesis and properties of the microballoon, have been still limited. In the early stage, the researches on polymeric microballoons were directed to the investigations of the effects of the existing microballoons on mechanical property of the foam (Lawrence et al , 2001; Mae et al, 2008 a, b and Gupta et al (2004)). Recently, some papers related to synthesis and expandability of the balloons. Kawaguchi et al. (2004 and 2005) developed a thermally expandable microballoon for foaming polypropylene (PP) that required high processing temperatures above 200°C. This temperature range cannot be accommodated by conventional thermally expandable microcapsules. Jonsson, et al., (2009; 2010) synthesized the microballoons and investigated the relation among their expandability, balloon size and the structure of crosslinker. Kawaguchi et al. (2010; 2011) consecutively investigated the expansion behavior of a conventional microballoon by visual inspection and developed a mathematical model for designing a new type of capsule. Their model consisted of Newtonian constitutive equation and equations for the diffusion and

evaporation of the blowing agent. The model shows fairly good but not complete agreement with experimental data. In particular, the elastic behavior of the balloon could not be simulated by the researchers' model.

In this study, the microballoon model was re-designed by considering the viscoelastic behavior of the shell to improve the predictability of the microballoon's expansion behavior both in air (free expansion) and in a polymer matrix.

2. MATHEMATICAL MODELS OF MICROBALLOON

2.1 Assumption for model development

A mathematical model was developed to describe the expansion behavior of a microballoon both in air and in a polymer matrix. It was considered that the expansion behavior comprises three basic phenomena: 1) deformation (expansion) of the polymeric shell, 2) evaporation of the liquid hydrocarbon blowing agent and establishment of a vapor pressure in the microballoon and 3) diffusion of the hydrocarbon blowing agent from the inside to the outside of the balloon.

Microscopy images of a microballoon before and after expansion are illustrated in Figure 1. From these images, a simple microballoon structure was constructed to have three major components: 1) a polymeric shell (outer layer), 2) a hydrocarbon liquid layer (middle layer)

and 3) a hydrocarbon gas phase (inner layer), as illustrated in Figure 2.

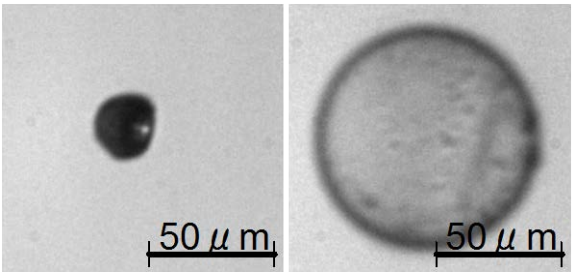

Figure 1 Microscopic images of microballoon (a) before expansion and (b) after foaming

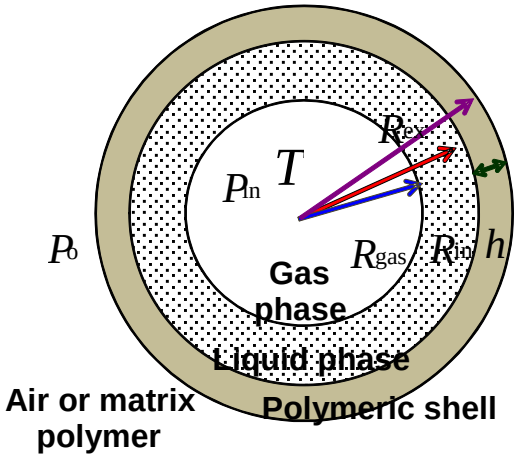

Figure 2 Schematic structure of microballoon

To develop a microballoon model, the following assumptions were made for the abovementioned microballoon structure:

a) The balloon expands uniformly along the radial direction. In other words, the radius of the balloon changes while maintaining the balloon's spherical shape.

b) The polymeric shell is deformed uniformly along the radial direction only without any degradation (reactions) or breakup. The polymer properties are not altered by expansion.

c) The change in the density of the polymer shell with temperature is negligible.

d) The heat transfer in the balloon is so fast that the temperature of the balloon can be considered to be uniform and equal to the temperature of the surrounding media.

e) The effect of inertia on the deformation and fluidization of the polymeric shell is negligible because of the low Reynolds number: Because the radius of the balloon is several micrometers and the viscosity of polymer is high, the Reynolds number could be considered to be low.

f) There is no stress distribution in the polymer shell. The stress in the shell is uniform.

g) The shell polymer and the matrix polymer are viscoelastic and incompressible

h) The blowing agents satisfy the ideal gas law

i) The permeability of the liquid in the shell polymer is negligible compared with that of the gas. Only the permeability of the gaseous blowing agent in the shell polymer is considered.

j) The driving force of the permeability of the gas in the polymeric shell is governed by the difference in the partial pressures of the blowing agent inside and outside of the balloon.

With these assumptions, three basic equations, i.e., an equation of continuity, a momentum balance equation and the material balance equation of the blowing agent, were

developed using a constitutive viscoelastic equation and the ideal gas law.

2.2 Model Equations of Free Expansion in Air

In the developmental stage of a microballoon, the expandability of the microballoon is experimentally tested in free-expansion mode: a specified number of microballoons are placed in a temperature- controlled transparent vessel, the vessel is heated to expand the balloons at a given temperature under atmospheric pressure and the volumetric change before and after expansion is measured. Therefore, we first developed a models of an isolated microballoon suspended in air to describe the expansion behavior during the course of heating.

2.2.1 Equation of Continuity

With the assumption of the incompressibility of the shell polymer (g), the equation of continuity of the polymer is given by

$$\nabla \cdot \mathbf{v} = 0 \tag{1}$$

Using spherical coordinates (r, θ, ϕ) and invoking assumption (b), the velocity of deformation or flow can be described by

$$\mathbf{v}(\mathbf{r}, t) = \mathbf{e}_{\mathrm{r}} v_{\mathrm{r}}(r, t) \quad \left(R_{\mathrm{in}}(t) \le r \le R_{\mathrm{ex}}(t)\right) \tag{2}$$

where $\mathbf{v}(\mathbf{r},t)$ is the velocity of the polymer at position $\mathbf{r} := (r,\theta,\phi)$ and time t. $v_r(r,t)$ is the radial component of the velocity at a radius r and at a time t. $\mathbf{e}_r$ is the unit vector along the radial direction. $R_{in}(t)$ and $R_{ex}(t)$ denote the inner radius of the polymer shell and the radius of the microballoon (outer radius), respectively, at time t, as illustrated in Fig. 2.

Because the shell polymer is incompressible (assumption (g)), $v_r(r,t)$ satisfies

$$\frac{1}{r^2}\frac{\partial}{\partial r}(r^2 v_r) = 0 \tag{3}$$

Taking the integral of Eq. (3), $v_r(r,t)$ can be expressed as an r-independent function $F(t)$:

$$v_r(r,t) = \frac{F(t)}{r^2} \tag{4}$$

Using the expressions $v_r(R_{in},t) = \dot{R}_{in}(t)$ and $v_r(R_{ex},t) = \dot{R}_{ex}(t)$, $F(t)$ can be derived from Eq. (4):

$$F(t) = R_{in}^2(t)\dot{R}_{in}(t) = R_{ex}^2(t)\dot{R}_{ex}(t) \tag{5}$$

In the above expressions and hereafter, the dot on a variable denotes the time derivative of the variable. Denoting the thickness of the polymeric shell by h (i.e., $R_{ex} = R_{in} + h$) and assuming that $R_{in} >> h$ is satisfied, Eq. (6) can be derived from Eq. (5) by neglecting the higher-order terms of h (i.e., h^2, h^3….,):

$$\frac{\dot{h}(t)}{h(t)} = -2\frac{\dot{R}_{in}(t)}{R_{in}(t)} \tag{6}$$

Integrating Eq. (6) yields

$$h(t)R_{in}^2(t) = V_0 \tag{7}$$

where V_0 is a constant volumetric parameter.

By introducing an expansion ratio, $\lambda(t) \equiv \frac{R_{in}(t)}{R_{in}^{(0)}}$, Eq. (7) can be rewritten as follows:

$$h(t) = h^{(0)} \lambda^{-2}(t) \tag{8}$$

where the superscript (0) indicates the initial value of the variable.

Eq. (8) is the equation of continuity for describing changes in the radius and thickness of the polymer shell.

2.2.2 Momentum Balance Equations:

The momentum balance equation for a microballoon is as follows:

$$\rho_s \left[\frac{\partial \mathbf{v}}{\partial t} + (\mathbf{v} \cdot \nabla)\mathbf{v} \right] = -\nabla p + \nabla \cdot \boldsymbol{\sigma} \tag{9}$$

where ρ_s, p, σ are the density, pressure and stress of the shell polymer, respectively.

By substituting Eqs. (2) and (4) into Eq. (9), the radial component of Eq. (9) is transformed into

$$\frac{\rho_s}{r^2} \left[\dot{F}(t) - \frac{2F^2(t)}{r^3} \right] = -\frac{\partial p}{\partial r} + [\nabla \cdot \boldsymbol{\sigma}]_r \tag{10}$$

Assumption (a) and (b) lead to $\sigma_{\theta r} = 0$ and $\sigma_{\varphi r} = 0$. Thus, the right-hand side of Eq. (10) can be rewritten as follows:

$$\frac{\rho_s}{r^2} [\dot{F}(t) - \frac{2F^2(t)}{r^3}] = -\frac{\partial p}{\partial r} + \frac{\partial \sigma_{rr}}{\partial r} + \frac{2\sigma_{rr} - \sigma_{\theta\theta} - \sigma_{\varphi\varphi}}{r} \tag{11}$$

Integrating both sides of Eq. (11) with respect to r from R_{in} to R_{ex} gives

$$\rho_s\left[-\left(\frac{1}{R_{ex}(t)}-\frac{1}{R_{in}(t)}\right)\dot{F}(t)+\left(\frac{1}{R_{ex}^4(t)}-\frac{1}{R_{in}^4(t)}\right)\frac{F^2(t)}{2}\right]=-p(R_{ex})+p(R_{in})+\sigma_{rr}\big|_{r=R_{ex}}-\sigma_{rr}\big|_{r=R_{in}}+\int_{R_{in}}^{R_{ex}}\left[\frac{2\sigma_{rr}-\sigma_{\theta\theta}-\sigma_{\varphi\varphi}}{r}\right]dr \tag{12}$$

The force balances at the inner and outer surfaces of the polymeric shell are as follows:

$$\text{At the inner surface}\quad P_{in}=p(R_{in})-\sigma_{rr}\big|_{r=R_{in}}+\frac{2\gamma}{R_{in}}=p(R_{in})-\sigma_{rr}\big|_{r=R_{in}}+\frac{2\gamma}{R_{in}^{(0)}\lambda} \tag{13}$$

$$\text{At the outer surface}\quad p(R_{ex})-\sigma_{rr}\big|_{r=R_{ex}}=P_o+\frac{2\gamma}{R_{ex}}=P_o+\frac{2\gamma}{R_{in}^{(0)}\lambda+h^{(0)}\lambda^{-2}} \tag{14}$$

where P_{in} and P_o, respectively, denote the pressure inside the balloon and that of the media (air or polymer) surrounding the balloon.

Using $R_{ex}=R_{in}+h$, $R_{in}>>h$ together with Eqs. (5) and (8), the right-hand side (*RHS*) of Eq. (12) can be simplified to

$$RHS\cong\rho_s\frac{h(t)}{R_{in}^2(t)}\left[\dot{F}(t)-\frac{2}{R_{in}^3(t)}F^2(t)\right]=\rho_s h^{(0)}R_{in}^{(0)}\frac{\ddot{\lambda}(t)}{\lambda^2(t)}$$

Using the notation $\Delta\sigma\equiv 2\sigma_{rr}-\sigma_{\theta\theta}-\sigma_{\varphi\varphi}$, taking the Taylor expansion and substituting Eq. (8), the last term of Eq. (12) (*LT Eq*(12)) can also be simplified to

$$LTEq.12=\int_{R_{in}}^{R_{ex}}\left[\frac{\Delta\sigma}{r}\right]dr\cong\frac{h^{(0)}}{R_{in}^{(0)}}\frac{\Delta\sigma\big|_{r=R_{in}}}{\lambda^3}$$

Then, neglecting the inertia, i.e., $\rho_p h^{(0)}R_{in}^{(0)}\frac{\ddot{\lambda}(t)}{\lambda^2(t)}$, Eq. (12) is finally transformed into

$$0=P_{in}-P_o-2\gamma\left(\frac{1}{R_{in}^{(0)}\lambda}+\frac{1}{R_{in}^{(0)}\lambda+h^{(0)}\lambda^{-2}}\right)+\frac{h^{(0)}}{R_{in}^{(0)}}\frac{\Delta\sigma\big|_{r=R_{in}}}{\lambda^3} \tag{15}$$

The stress difference in Eq. (15), $\Delta\sigma$, can be calculated by the following constitutive equation for a viscoelastic shell polymer.

2.2.3 Constitutive Equation (Stress-Deformation)

The viscoelasticity of the shell polymer is described by the upper convective Maxwell model:

$$\boldsymbol{\sigma} + \tau \overset{\nabla}{\boldsymbol{\sigma}} = 2\eta \mathbf{D} \tag{16}$$

where, $\overset{\nabla}{\boldsymbol{\sigma}} = \dot{\boldsymbol{\sigma}} + (\boldsymbol{v}\cdot\nabla)\boldsymbol{\sigma} - (\nabla \boldsymbol{v})\cdot\boldsymbol{\sigma} - \boldsymbol{\sigma}\cdot(\nabla \boldsymbol{v})^{\mathrm{T}}$ $\boldsymbol{\sigma}$ is the stress tensor, and η is the shear viscosity. G ~~is~~ the shear elastic modulus~~.~~ $\tau = \eta/G$ is the relaxation time. $\mathbf{D}$ is the deformation rate tensor, and $\nabla\mathbf{v}$ is the velocity gradient tensor. The temperature dependences of G, η and τ are addressed by the Arrhenius type equations $\mathrm{G} = A_G \exp\left(B_o/T\right)$ and $\tau = A_\tau \exp\left(B_\tau/T\right)$. T is the temperature of the microballoon.

Assuming that no stress exists in the balloon shell before expansion (assumption (f)), rearranging Eq. (16) using Eq. (5) gives the following equation for each element of Eq. (16)

$$\frac{d\sigma_{rr}}{dt} = -4(\sigma_{rr} + G)\frac{\dot{\lambda}}{\lambda} - \frac{\sigma_{rr}}{\tau}$$
$$\frac{d\sigma_{\theta\theta}}{dt} = 2(\sigma_{\theta\theta} + G)\frac{\dot{\lambda}}{\lambda} - \frac{\sigma_{\theta\theta}}{\tau} \tag{17}$$

$$\frac{d\sigma_{\varphi\varphi}}{dt} = 2(\sigma_{\varphi\varphi} + G)\frac{\dot{\lambda}}{\lambda} - \frac{\sigma_{\varphi\varphi}}{\tau}$$

Then, $\Delta\sigma$ can be calculated by

$$\frac{d\Delta\sigma}{dt} = (2\Delta\sigma - 12\sigma_{rr} - 12G)\frac{\dot{\lambda}}{\lambda} - \frac{\Delta\sigma}{\tau} \tag{18}$$

2.2.4 Material Balances of Blowing Agent

A mixture of hydrocarbons is often used as the blowing agent. The model was developed to accommodate not only single but also multiple hydrocarbon components. From assumption (h), the pressure inside the microballoon is established by the vapor pressure of the hydrocarbon and can be determined by

$$P_{in} = \sum_k P_k = \sum_k \frac{m_{yk}}{M_k} RT\left(\frac{4\pi}{3}R_{gas}^3\right)^{-1} \tag{19}$$

where P_k is the partial pressure of the k^{th} component of the blowing agent. M_k is the molecular weight of the k^{th} component of the blowing agent, and R is the universal gas constant. m_{yk} is the mass of the blowing agent in the gas phase. R_{gas} is the radius of the gas phase in the microballoon, as illustrated in Fig. 2.

The total volume of the balloon core should be equal to the sum of the volumes of the gas and liquid phases, as shown in Fig. 2:.

$$\frac{4\pi}{3}R_{in}^{(0)3}\lambda^3 = \frac{4\pi}{3}R_{gas}^3 + \sum_k \frac{m_{xk}}{\rho_{Lk}} \tag{20}$$

where ρ_{Lk} is the liquid density of the k^{th} component of the blowing agent and m_{xk} is the mass of the k^{th} component of the blowing agent in the liquid phase.

The evaporation rate is a function of the saturation pressure, P_{sat}, of the blowing agent at temperature T:

$$\frac{dm_{xk}}{dt} = -4\pi R_{gas}^2 k_{mk}\left(P_{sat} - P_k\right) \tag{21}$$

where k_{mk} is the mass transfer coefficient of the k^{th} component of the blowing agent. The saturation pressure, $P_{sat,k}$, of the k^{th} component of the blowing agent is temperature-dependent and is given by the Antoine equation and Raoult's law (assumption (h)):

$$P_{sat\,k} = \frac{m_{xk}/\mathrm{M}_k}{\sum_l \left(m_{xl}/\mathrm{M}_l\right)} \exp\left(A_k - \frac{B_k}{T + C_k}\right) \tag{22}$$

where A_k, B_k and C_k are the property parameters of the k^{th} component of the blowing agent

The blowing agent permeates the polymer shell and diffuses from the balloon after its liquid phase disappears (assumptions (i) and (j)). The mass flow rate from the inside to the outside of the microballoon is given by

$$\frac{dm_{zk}}{dt} = 4\pi R_{in}\left(R_{in} + h\right)\frac{k_{pk}}{h} P_k = 4\pi \frac{R_{in}^{(0)}}{h^{(0)}}\left(R_{in}^{(0)}\lambda^4 + h^{(0)}\lambda\right) k_{pk} P_k \tag{23}$$

where $k_{p,k}$ is the permeability coefficient and $4\pi R_{in}\left(R_{in} + h\right)$ is the average shell surface area. m_{zk} is the weight of the blowing agent diffusing from the balloon.

The total mass balance of the k^{th} component of the blowing agent is given by

$$m_{xk} + m_{yk} + m_{zk} = m_{xk}^{(0)} + m_{yk}^{(0)} + m_{zk}^{(0)} \tag{24}$$

2.3 Model Equations of Expansion in Polymer

As mentioned before, the performance of a microballoon is often evaluated by conducting an expansion test in air. However, in practice, the balloon is used by blending with thermoplastic polymers to foam the polymers. Therefore, it is also important to develop models describing the expansion behavior of a balloon in a polymer matrix. The free-expansion models for a microballoon could be extended to describe the foaming behavior in a polymer matrix with some modifications of the momentum balance and material balance equations.

2.3.1 Momentum Balance Equations:

When the microballoon is placed in a polymer matrix, Eq. (11) must be integrated over the range $[R_{in}, R_{ex}]$ for a microballoon and over the range $[R_{ex}, \infty]$ for the polymer matrix that surrounds the microballoon.

$$0 = -p_s(R_{ex}) + p_s(R_{in}) + \sigma_{rrs}\big|_{r=R_{ex}} - \sigma_{rrs}\big|_{r=R_{in}} + \int_{R_{in}}^{R_{ex}} \left[\frac{2\sigma_{rrs} - \sigma_{\theta\theta s} - \sigma_{\varphi\varphi s}}{r} \right] dr \tag{25}$$

$$0 = -p_p(r \to \infty) + p_p(R_{ex}) + \sigma_{rrp}\big|_{r\to\infty} - \sigma_{rrp}\big|_{r=R_{ex}} + \int_{R_{ex}}^{\infty} \left[\frac{2\sigma_{rrp} - \sigma_{\theta\theta p} - \sigma_{\varphi\varphi p}}{r} \right] dr \tag{26}$$

where subscript s and p stand for the variables related to shell polymer and polymer surrounding the microballoon (matrix polymer), respectively.

As a boundary condition, the force balances at the interface between the balloon and matrix polymer and at the inner surface of the polymeric shell (i.e., interface between polymer and gas) are, respectively, given by

$$P_{\mathrm{in}} = p_{\mathrm{s}}(R_{\mathrm{in}}) - \sigma_{\mathrm{rrs}}\big|_{r=R_{\mathrm{in}}} + \frac{2\gamma_{\mathrm{s}}}{R_{\mathrm{in}}} = p_{\mathrm{s}}(R_{\mathrm{in}}) - \sigma_{\mathrm{rrs}}\big|_{r=R_{\mathrm{in}}} + \frac{2\gamma_{\mathrm{s}}}{R_{\mathrm{in}}^{(0)}\lambda} \tag{27}$$

$$\begin{aligned} p_{\mathrm{s}}(R_{\mathrm{ex}}) - \sigma_{\mathrm{rrs}}\big|_{r=R_{\mathrm{ex}}} &= p_{\mathrm{p}}(R_{\mathrm{ex}}) - \sigma_{\mathrm{rrp}}\big|_{r=R_{\mathrm{ex}}} + \frac{2\gamma_{\mathrm{sp}}}{R_{\mathrm{ex}}} \\ &= p_{\mathrm{p}}(R_{\mathrm{ex}}) - \sigma_{\mathrm{rrp}}\big|_{r=R_{\mathrm{ex}}} + \frac{2\gamma_{\mathrm{sp}}}{R_{\mathrm{in}}^{(0)}\lambda + h^{(0)}\lambda^{-2}} \end{aligned} \tag{28}$$

where γ_{s} and γ_{sp} are the surface tension of the shell polymer and the interfacial tension between the shell polymer and the matrix polymer.

Considering that the pressure of the matrix polymer at bulk $p_{\mathrm{p}}(r\to\infty)$ is constant, P_{o}, the distance over which the polymer is deformed is negligible, i.e., $\sigma_{\mathrm{rrp}}\big|_{r\to\infty} = 0$ at an infinite distance from the center of the balloon. Thus, the overall force balance around a microballoon in a polymer matrix is given by

$$0 = \left(P_{\mathrm{in}} - P_{\mathrm{o}}\right) - \left(\frac{2\gamma_{\mathrm{s}}}{R_{\mathrm{in}}} + \frac{2\gamma_{\mathrm{sp}}}{R_{\mathrm{ex}}}\right) + \int_{R_{\mathrm{in}}}^{R_{\mathrm{ex}}} \left[\frac{\Delta\sigma_{\mathrm{s}}}{r}\right] dr + \int_{R_{\mathrm{ex}}}^{\infty} \left[\frac{\Delta\sigma_{\mathrm{p}}}{r}\right] dr \tag{29}$$

The constitutive equation for the shell polymer and that for the matrix polymer are, respectively, given by:

$$\frac{d\sigma_{rr}}{dt} = -4(\sigma_{rr} + G)\frac{\left(R_{in}^{(0)}\right)^3 \lambda^2 \dot{\lambda}}{\zeta + \left(R_{in}^{(0)}\right)^3 \lambda^3} - \frac{\sigma_{rr}}{\tau} \tag{30}$$

$$\frac{d(\Delta\sigma)}{dt} = (2\Delta\sigma - 12\sigma_{rr} - 12G)\frac{\left(R_{in}^{(0)}\right)^3 \lambda^2 \dot{\lambda}}{\zeta + \left(R_{in}^{(0)}\right)^3 \lambda^3} - \frac{\Delta\sigma}{\tau} \tag{31}$$

where $\zeta = r^3 - R_{in}^3$.

To calculate σ_{rr} and $\Delta\sigma$ in the shell, ζ must be taken from 0 to $R_{ex}^3 - R_{in}^3$ and G should be chosen as the shear elastic modulus of the shell polymer. To calculate σ_{rr} and $\Delta\sigma$ in the matrix polymer using Eqs. (30) and (31), ζ is taken from $R_{ex}^3 - R_{in}^3$ to infinity (a certain distance in the simulation) and G and τ are chosen as the elastic moduli of the matrix polymer. The temperature dependences of G and τ for the matrix polymer are also obtained using Arrhenius-type equations: $G = A_{GP}\exp\left(B_{oP}/T\right)$ and $\tau = A_{\tau P}\exp\left(B_{\tau P}/T\right)$.

2.3.2 Material Balances of blowing agent:

Eqs. (18)-(22) and (24) can be applied to the case in which the microballoon is placed in a polymer matrix. Eq. (23) should be modified to calculate the concentration profiles of the blowing agent in the polymer matrix as well as the mass transfer of the agent by diffusion.

Assuming that the diffusion of the k^{th} component of the blowing agent follows Fick's laws and does not affect the diffusion mechanisms of the other components, the following mass balance equations are satisfied.

$$\frac{dz_k}{dt} = \frac{d}{dt}\int_{R_{ex}}^{\infty}\left(4\pi r^2 M_k c_k\right)dr = -4\pi R_{ex}^2 D_{eff,k} M_k \left(\frac{\partial c_k}{\partial r}\right)\Bigg|_{r=R_{ex}}$$

$$= 4\pi R_{ex} R_{in} \frac{k_{pk}}{h}\left(P_k - P_{ex,k}\right) \tag{32}$$

where $D_{eff,k}$ is the diffusion coefficient of the kth component of the blowing agent in the matrix polymer. $P_{ex,k}$ is the equilibrium pressure of the kth component of the blowing agent at the interface between the shell polymer and the matrix polymer.

In this study, to reduce the calculation burden of simulation, the concentration profile of the kth component of the blowing agent at the outer surface of the shell was obtained by an integral approximation (Rosner and Epstein, 1972) without solving the partial differential equation of Fick's second law:

$$c_k = \begin{cases} c_{R,k}\left(\dfrac{R_{ex}+\delta-r}{\delta}\right)^2 & R_{ex} \le r \le R_{ex}+\delta \\ 0 & R_{ex}+\delta \le r \end{cases} \tag{33}$$

where δ is a hypothetical thickness of the concentration profile. c_{Rk} is the equilibrium concentration of the k^{th} component of the blowing agent at the interface between the shell polymer and the matrix polymer.

Based on the assumption that the blowing agent follows Henry's law (Eq. (34)), c_{Rk} is calculated as follows:

$$c_{Rk} = P_{ex,k} k_{H,k}^{-1} \tag{34}$$

where $k_{H,k}$ is the Henry's constant.

From Eqs. (32)-(34), the concentration gradient of the kth component of the blowing agent is derived as follows:

$$\left(\frac{\partial c_k}{\partial r}\right)_{R_{ex}} = -\frac{2c_{Rk}}{R_{ex}}\left(-1+\sqrt{1+\frac{3}{2\pi M_k R_{ex}^3}\frac{z_k}{c_{Rk}}}\right)^{-1} \tag{35}$$

where c_{Rk} is the concentration of the kth component of the blowing agent at the interface between the shell polymer and surrounding polymer.

As illustrated in Figure 3, the mass balance is satisfied at the interface between the shell polymer and the surrounding polymer for each component of the blowing agent.

$$-4\pi R_{ex}^2 D_{eff,k} M_k \left(\frac{\partial c_k}{\partial r}\right)_{r=R_{ex}} == 4\pi R_{ex} R_{in} \frac{k_{pk}}{h}\left(P_k - P_{ex,k}\right) \tag{36}$$

$P_{ex,k}$ can be calculated by solving the following algebraic equation, which is derived by substituting Eqs. (34) and (35) into (36).

$$2\frac{P_{ex,k}}{k_{H,k}} D_{eff,k} M_k \left(-1+\sqrt{1+\frac{3k_{Hk}}{2\pi M_k R_{ex}^3}\frac{z_k}{P_{ex,k}}}\right)^{-1} = R_{in}\frac{k_{pk}}{h}\left(P_k - P_{ex,k}\right) \tag{35}$$

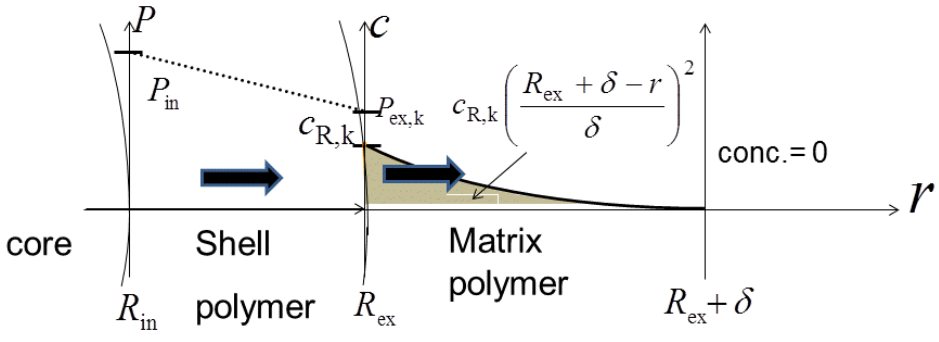

Figure 3 Concentration profile and mass transfer at the interface between microballoon and matrix polymer

3. VISUAL OBSERVATION EXPERIMENTS AND SIMULATION RESULTS

To determine the unknown parameters and confirm the predictability of the developed models, an experiment performed by visual inspection was conducted using the set-up illustrated in Figure 4.

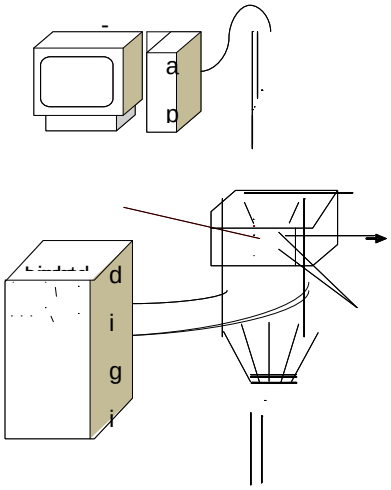

Figure 4 Experimental set-up used to observe microballoon expansion

A microballoon was placed in a view cell, which features two sapphire windows on both of its walls; the size of the cell is given elsewhere. Then, the balloon was heated by electrical heaters to a specified temperature. With the optical light source behind one of the windows, the expansion behavior of the balloon was observed through the other window by a high-speed camera.

Figure 5 compares the expansion behavior of the microballoon observed by visual inspection with that predicted by the simulation. The experimental conditions are listed in Table 1. The visual observation experiments were conducted by heating an acrylonitrile-based microballoon[1,7] in the view cell from 80 to 220 °C. The blowing agent in the balloon was an 86:14 mixture of i-pentane and n-octane. The black dotted line and the black solid line represent the temperature profile and the change in the radius of the expanding microballoon, respectively. The expansion ratio was given by the ratio of the radius at time t to the initial radius of the microballoon.

The values of the model parameters are given in Table 2. In the simulation, both hydrocarbon blowing agents had the same mass transport coefficients ($k_{m1} = k_{m2}$) and permeability coefficients ($k_{p,1} = k_{p,2}$). The values of $k_{m,k,}$ and $k_{p,k}$, and the rheological parameters, A_G and A_τ, were determined such that the simulation calculation would fit the experimental data as close as possible. Other parameters were obtained from the references. When the expansion behavior was calculated, the experimentally-obtained temperature was approximated and simulated by a ramp function and the simulated temperature was imposed to the simulation program.

Table 1 Experimental conditions of microballoon in air

Base Resin of Balloon	Acrylonitrile-based resin [1]
Blowing Agent	i-pentane/ n-octane
Surrounding Media	Air
Processing Temperature	80 – 220 ^{o}C

Table 2 Simulation Parameters (balloon in air)

Ambient Pressure [kPa]	101.3	ρ_L[kg m^{-3}] of octane	702.8
Surface tension [Pa m]	0.018	Mw [kg mol^{-1}]of octane	0.11423
Initial radi $R_{in}^{(0)}$ [μm]	6.6	ρ_L[kg m^{-3}] of pentane	626.38
Initial $h(0)$ [μm]	2.0	Mw [kg mol^{-1}]of pentane	0.07215
km,k [kgPa^{-1}m^{-2}s^{-1}]	1.0x10^{-7}	Weight ratio of blowing agent to balloon [-]	0.3
kp,k [kgPa^{-1}m^{-1}s^{-1}]	6.0x10^{-20}	Pentane / Octane ratio [-]	86:14
A_G of shell polymer G [Pa]	3.65x10^{-13}	A_τ of shell polymer τ [s]	7.714*10^{-5}
B_G of shell polymer G[Pa]	20139	B_τ of shell polymer τ [s]	6863.8
A of Antoine Eq. of octane	205778	A of Antoine Eq. of pentane	20.7261
B of Antoine Eq. of octane	2896.28	B of Antoine Eq. of pentane	2477.07
C of Antoine Eq. of octane	52.41	C of Antoine Eq. of pentane	39,94

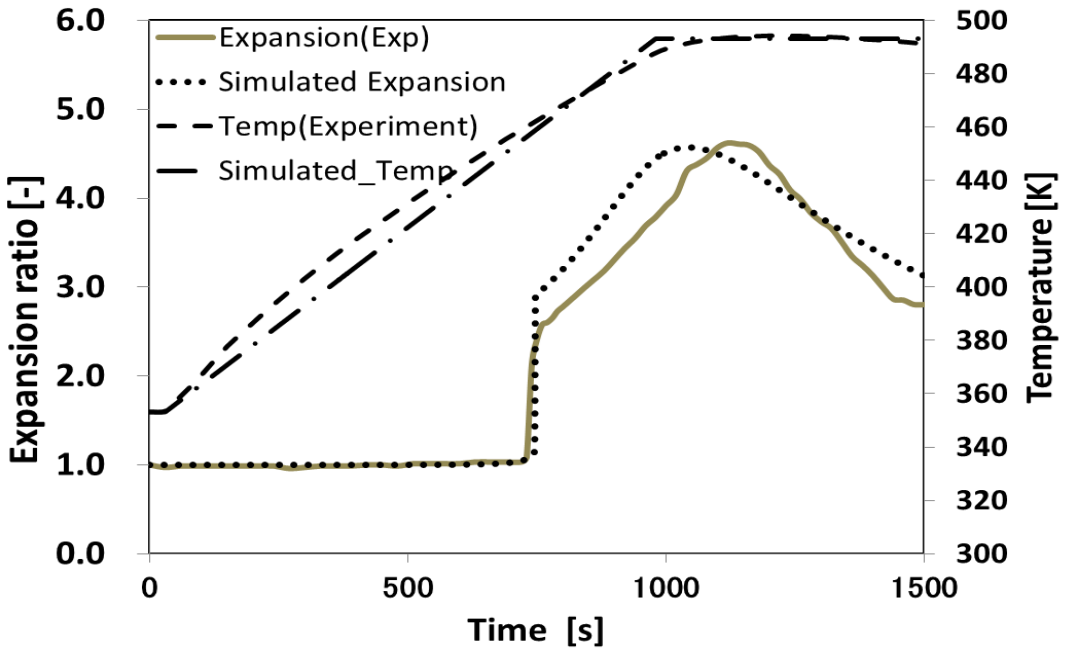

Figure 5 Experimental and simulation results of microballoon expanding in air

Even though the fitting parameters were still needed, the expansion behavior of the microballoon described by the developed models was in good agreement with the observed behavior. In particular, the temperature at which the microballoon began expanding was exactly the same as that observed in the experiment. The elastic behavior of the expanding microballoon was also expressed by the simulation. The shrinkage of the microballoon induced by gas escape was simulated even though there was a discrepancy in the rate of shrinkage between the experiment and simulation.

The discrepancy in shrinkage behavior might be caused by the incompleteness of modeling the diffusion process: In the real process, a mass transfer of the liquid blowing agent in polymer shell may occur, the phase transition of the blowing agent from liquid to gas may occur in the polymer shell. In addition, the replacement of the gaseous blowing agent with air might occur. Those phenomena could not be expressed by the present models.

Figure 6 compares the expansion behavior of the microballoon in a polymer matrix observed by experiment with that described by the simulation. The visual observation experiments were conducted by heating the same microballoon that we used in the free-expansion experiments (expansion in air). Most of the model parameters describing the

microballoon were the same as those presented in Table 2, except for the rheological properties. The rheological parameters of the matrix polymer (polystyrene) were tuned to make the simulated expansion behavior as close to the experimental profile as possible. The resulting model parameters are listed in Table 3. The black and red solid lines represent the experimental and simulated expansion behavior of the microballoon, respectively. Due to the presence of a matrix polymer, the expansion behavior was suppressed and the shrinkage rate was reduced to some extent compared with the expansion behavior in air. The simulation successfully described the observed expansion and shrinkage behaviors.

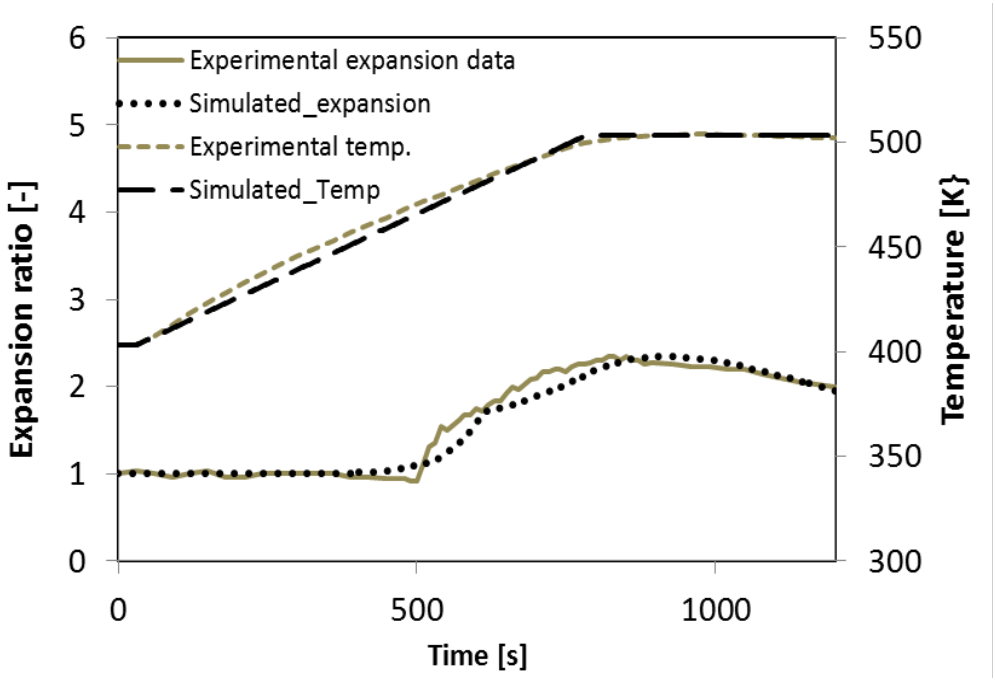

Figure 6 Experimental and simulation results of microballoon expanding in polystyrene

Table 3 Experimental conditions and simulation parameters (balloon in polymer)

Base resin of balloon	acrylonitrile	Matrix polymer	Polystyrene
Matrix polymer	0.018	Weight ratio of blowing agent	0.2
Ambient Press [kPa]	101.3	Temp [^{o}C]	130 - 230
$D_{eff,k}$ [$m^2 \cdot s^{-1}$]	$1.0x10^{-13}$	Henry const. $k_{H,1} = k_{H,2}$	$1.0*10^{-2}$
A_G of shell polymer G [Pa]	$4.56x10^{-13}$	A_τ of shell polymer τ [s]	$7.714*10^{-5}$
B_G of shell polymer G[Pa]	20139	B_τ of shell polymer τ [s]	6863.8
A_{Gp} of matrix polymer G [Pa]	$3.65x10^{-13}$	A_τ of matrix polymer τ [s]	$7.714*10^{-5}$
B_{Gp} of matrix polymer G[Pa]	20139	B_τ of matrix polymer τ [s]	6863.8
δ [μm]	13 h(t)		

4. SENSITIVITY ANALYSIS

Using the developed model, a sensitivity analysis was conducted to determine the effect of elasticity, the relaxation time of the shell polymer, and the permeability of the blowing agent on the expansion behavior. For the analysis, the mathematical model of free expansion (in air) with a single-component blowing agent (pentane) was used. The values of the model parameters are presented in Table 4. Figure 7 shows the expansion behaviors of the balloon with the different elasticity of the shell polymer. The balloon expansion ratio was defined by the ratio of the radius of the balloon at time t to the initial radius. As the elastic modulus of the shell polymer increased, the onset temperature of expansion was shifted to higher temperatures and the degree of initial deformation of the microballoon was reduced. Furthermore, the maximum expansion ratio was increased with the increase in elastic

modulus. These behaviors could be explained in the following way: because of the increase in the onset temperature of expansion, the difference between inside and outside pressures at the onset, which is the driving force of balloon growth, was increased and as a result, the degree of the balloon deformation (expansion) was increased.

Table 4 Model Parameter values for sensitivity analysis

Base resin of balloon	acrylonitrile	Blowing agent (BA)	Pentane
Shell density .[kg m^{-3}]	810	Pentane / Octane ratio	100:0
Temperature condition	From 80 to 220 C	Mw[$kgmol^{-1}$] pentane	0.07215
Ambient Pressure [kPa]	101.3	weight ratio of BA	0.3
Surface tens. [Pa m]	0.018	Liquid dens ρ_L[kg m^{-3}]	626.38
Initial radi $R_{in}^{(0)}$ [μm]	6.6	km,1 [$kgPa^{-1}m^{-2}s^{-1}$]	$1.0x10^{-7}$
Initial $h(0)$ [μm]	2.0	kp,1[$kgPa^{-1}m^{-1}s^{-1}$]	$6.0x10^{-20}$
A_G of shell polymer G [Pa]	$3.2843x10^{-13}$	A_τ of shell polymer τ [s]	$3.857*10^{-5}$
B_G of shell polymer G[Pa]	20139	B_τ of shell polymer τ [s]	6863.8
A of Antoine Eq. of pentane	20.7261	B of Antoine Eq. of pentane	2477.07
C of Antoine Eq. of pentane	39,94		

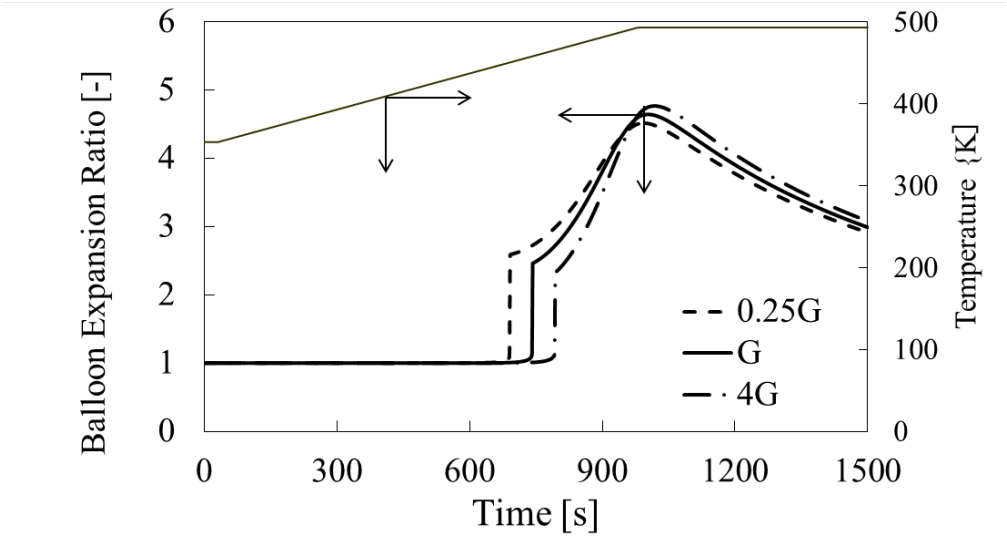

Figure 7 Effect of elastic modulus of shell polymer on expansion behavior

Figure 8 shows the effect of the relaxation time of the shell polymer on microballoon expansion; the simulation was carried out by changing the relaxation time τ of the shell polymer. As shown, the temperature required to reach the maximum expansion ratio increased and the amplitude of the maximum expansion ratio decreased as the relaxation time increased.

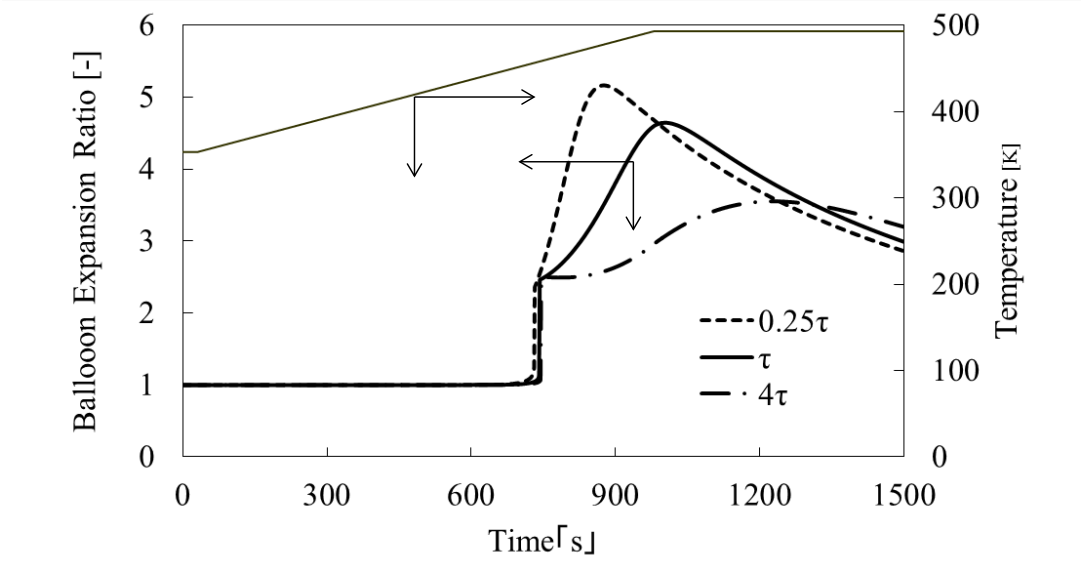

Figure 8 Effect of relaxation time on expansion behavior

Figure 9 shows the effect of the permeability of the gaseous blowing agent in the shell polymer, $k_{p,k}$, on the expansion behavior. The simulation was carried out by changing the permeability of the blowing agent in the shell polymer. The effect of the permeability was prominent. As the permeability increased, the maximum expansion ratio was reduced and the size of the microballoon quickly decreased.

From the sensitivity analysis, the following microballoon design strategy could be

established: to increase the expansion temperature, the elastic modulus of the shell polymer must be increased. To increase the maximum expansion ratio, the relaxation time and permeability must be reduced. The permeability should be reduced to prevent the microballoon from shrinking quickly and maintain the dimensional stability of the resulting foams.

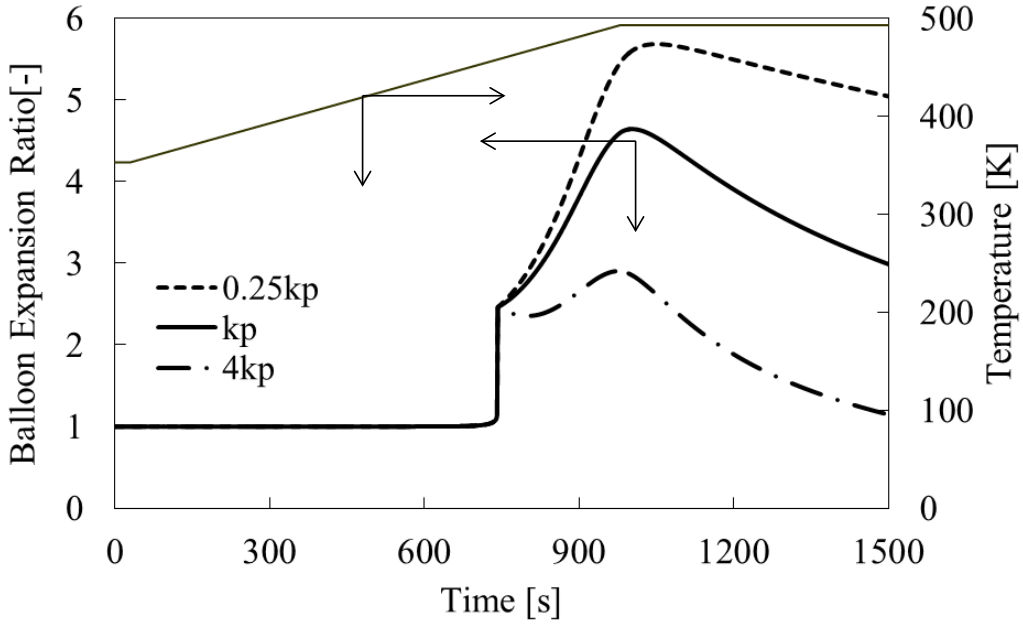

Figure 9 Effect of permeability on expansion behavior of microballoon

5. CONCLUSIONS

A mathematical model was developed to describe the expansion behavior of a microballoon in air and in a polymer matrix. Because some of the physical properties of the microballoon, such as the viscosity of the shell polymer, were not experimentally available,

estimates were used for the simulation. Those estimates may induce some discrepancy between the simulation and experimental results. However, the present model was able to describe the intrinsic expansion behavior of a microballoon. For example, as the relaxation time of the shell polymer increased, the amplitude of the expansion ratio decreased and the expansion behavior was decelerated. Similar behavior was observed when the permeability coefficient of the shell polymer increased. When the permeability of the blowing agent in the shell polymer increases, the shrinkage of the balloon becomes prominent. To reduce the degree of shrinkage, crosslinking could be employed. However, crosslinking also increases the elastic modulus of the shell polymer and reduces the degree of initial expansion. The models are not perfect at the present stage but they can be used to optimize microballoon design semi-quantitatively. For further improvements of the simulation accuracy, the additional models are needed to describe the phenomena that air, N_2 and CO_2 diffuse into the expanding balloon from outside or surrounding polymer. The values of physical parameters adjusted for the simulation calculations might be different from the true values of the materials. To develop the sophisticated models and perform the simulation without fitting the model parameters, the precise measurements of the physical parameters, such as diffusion coefficients and mass transfer coefficients, are needed

References

Ahmad, M., Flexible Vinyl Resiliency Property Enhancement with Hollow Thermoplastic Microspheres, 2001, Vinyl & Additive Technol., 7(3), 156-161 .

D'Agostino, D., Takacs, E., and Vlachopoulos, J., The Effect of Coupling Agents on foaming with Polymer Microsphere in Rotational Molding, 2003, SPE ANTEC Tech. Papers, 49, 1205-.1208

Gupta, N. and Woldensenbet, E., Microballoon Wall Thickness Effects on Properties of Syntactic Foams, 2004, J. of Cellular Plastics, 40, 461-480

Mae, H., Tensile mechanical properties in PP/SEBS/microballoon composites under impact loading, Journal of Achievements in Materials and Manufacturing Engineering, 2008, 31 (2) 341-347

Mae, H., Relationship of Mechanical Properties between Neat PP/SEBS Blends and Syntactic PP/SEBS Foams with Polymer Microballoons, 2008, J. of the Society of Materials Science, 57(12) 1253-1260

Jonsson, L., Expandable microspheres as foaming agent in thermoplastics, thermosets and elastomers, Proc. of Blowing Agents and Foaming Processes,2006 ,May, Germany, paper 3, 1-8

Jonsson, M., Nordin, O., Kron, A-L, Malmstrom, E., Thermally Expandable Microspheres

with Excellent Expansion Characteristics at High Temperature, J. of Applied Polymer Science, 2010, 117, 384-392

Jonsson, M., Nystrom D., Nordin, O., Malmstrom, E., Surface modification of thermally expandable microspheres by grafting poly(glycidyl methacrylate) using ARGET ATRP, European Polymer Journal, 2009, 45, 2374-2382

Jonsson, M., Thermally Expandable Microspheres Prepared via Suspension Polymerization Synthesis, Characterization and Application, Trita-Che report 2010:4 KTH Chemical Science and Engineering,

Kawaguchi, Y., Oishi, T., Synthesis and properties of thermoplastic expandable microspheres: The relation between crosslinking density and expandable property, J. App. Polym. Sci, 2004, 93(2), 505-512

Kawaguchi, Y., Itamura, Y., Orimura, K., Oishi, T., Effects of the chemical structure on the heat resistance of thermoplastic expandable microspheres, J. App. Polym. Sci, 2005, 96 (4), 1306-1312

Kawaguchi, Y., Ohshima,M., Tanida, M., Ohishi, T., Ito, A., Sawa,T., 2011, Development of thermally expandable microcapsule and their mathematical models for polymer foaming, Seikei-Kakou, Vol.23, No.10, 627-635

Kawaguchi, Y., Ito, D., Kosaka, Y., Okudo, M., Nakachi, T., Kake, H., Kim, J.K., Shikuma, H.,

Ohshima, M., 2010, Thermally expandable microcapsules for polymer foaming-Relationship between expandability and viscoelasticity, Polymer Engineering and Science, 50, 4, 835-842

Morehouse, D. S.J., Tetreault, R.J., 1964, US Pat.3615972

Lundqvist, J.1992, Eur. Pat. 0486 080 B1

Yokomizo, T. , Tanaka, K, Niinuma, K, 1997, Jpn Pat. 9 019 635

Takacs, E., Vlachopoulos, J., and Rosenbusch, C., Foaming with Microspheres in Rotational Molding, 2002, SPEANTEC Tech. Papers, 48, 1271-1275

Taki, K., Nakayama, T., Yatsuzuka, T., Ohshima, M., 2003, Visual Observations of Batch and Continuous Foaming Processes, J of Cellular Plastics, 139, 2, 155-169

Rosner, D.E. and Epstein, M., Effects of interface kinetics, capillarity and solute diffusion on bubble growth rates in highly supersaturated liquids, 1972, Chem. Eng. Sci., 27(1), 69-88

Figure 1 Microscopic images of microballoon (a) before expansion and (b) after foaming

Figure 2 Schematic structure of microballoon

Figure 3 Concentration profile and mass transfer at the interface between microballoon and matrix polymer

Figure 4 Experimental set-up used to observe microballoon expansion

Figure 5 Experimental and simulation results of microballoon expanding in air

Figure 6 Experimental and simulation results of microballoon expanding in polystyrene